Article

TRANSPARENT PROCESS

THE EMBO JOURNAL

Lysophosphatidic acid acts as a nutrient-derived developmental cue to regulate early hematopoiesis

Haisen Li[1,†], Rui Yue[1,2,†], Bin Wei[1], Ge Gao[3], Jiulin Du[4] & Gang Pei[1,5,*]

Abstract

Primitive hematopoiesis occurs in the yolk sac blood islands during vertebrate embryogenesis, where abundant phosphatidylcholines (PC) are available as important nutrients for the developing embryo. However, whether these phospholipids also generate developmental cues to promote hematopoiesis is largely unknown. Here, we show that lysophosphatidic acid (LPA), a signaling molecule derived from PC, regulated hemangioblast formation and primitive hematopoiesis. Pharmacological and genetic blockage of LPA receptor 1 (LPAR1) or autotoxin (ATX), a secretory lysophospholipase that catalyzes LPA production, inhibited hematopoietic differentiation of mouse embryonic stem cells and impaired the formation of hemangioblasts. Mechanistic experiments revealed that the regulatory effect of ATX-LPA signaling was mediated by PI3K/Akt-Smad pathway. Furthermore, during *in vivo* embryogenesis in zebrafish, LPA functioned as a developmental cue for hemangioblast formation and primitive hematopoiesis. Taken together, we identified LPA as an important nutrient-derived developmental cue for primitive hematopoiesis as well as a novel mechanism of hemangioblast regulation.

Keywords embryonic stem cell; hemangioblast; hematopoiesis; LPA; zebrafish
Subject Categories Development & Differentiation; Signal Transduction
DOI 10.15252/embj.201387594 | Received 4 December 2013 | Revised 24 March 2014 | Accepted 10 April 2014 | Published online 14 May 2014
The EMBO Journal (2014) 33: 1383–1396

Introduction

The first wave of hematopoiesis, or primitive hematopoiesis, occurs in the yolk sac blood islands, which is initiated by mesodermal progenitor cells called hemangioblasts that can give rise to both primitive erythrocytes and endothelial cells through asymmetric cell division (Fehling *et al*, 2003; Orkin & Zon, 2008). The hemangioblasts were initially characterized *in vitro* using the hematopoietic differentiation model of mouse embryonic stem cells (mESCs) (Kennedy *et al*, 1997; Choi *et al*, 1998) and have been more recently identified in the primitive streak of the mouse embryo (Huber *et al*, 2004). The hemangioblasts exist at a very low frequency and are only detectable in a very short period of time during embryogenesis with the well-known cell-surface marker fetal liver kinase 1 (Flk1) (Ema *et al*, 2003; Huber *et al*, 2004). Previously, transcription factors such as Smad1, Scl, Lmo2, Fli1, and Gata2 were shown to regulate the formation of hemangioblasts (Warren *et al*, 1994; Gering *et al*, 2003; Lugus *et al*, 2007; Qian *et al*, 2007; Zafonte *et al*, 2007; Liu *et al*, 2008). Bone morphogenetic protein 4 (BMP4), fibroblast growth factor (FGF), hedgehog, and vascular endothelial growth factor (VEGF) were also demonstrated to regulate the induction of hemangioblasts (Damert *et al*, 2002; Park *et al*, 2004; Hochman *et al*, 2006; Walmsley *et al*, 2008); however, whether lipid molecules or G protein-coupled receptor (GPCR) signaling can play equally important roles in hemangioblast regulation is still elusive.

The yolk sac contains a large amount of phospholipids such as phosphatidylcholines (PC) to provide nutrition for the developing embryo (Noble & Moore, 1967; Fisher *et al*, 2002; Freyer & Renfree, 2009). PC are hydrolyzed into lysophosphatidylcholine (LPC) by secreted phospholipase A2 (sPLA2) (Schmitz & Ruebsaamen, 2009), and LPC is further hydrolyzed into LPA by the secretory lysophospholipase ATX (Tokumura *et al*, 2002; Umezu-Goto *et al*, 2002). LPA is an important signaling molecule that functions by activating its cognate GPCR (Anliker & Chun, 2004). So far, six subtypes of LPA receptor have been identified (LPAR1-6). *Lpar1*-deficient mice exhibit neonatal lethality partially due to defective suckling (Contos *et al*, 2000), while *lpar3*-deficient mice show anomalous embryo spacing and delayed blastocyst implantation (Freyer & Renfree, 2009). In contrast, both *lpar2*- and *lpar4*-deficient mice are grossly normal (Estivill-Torrus *et al*, 2008; Lee *et al*, 2008). Interestingly, *atx*-deficient mice died at embryonic day 9.5 with profound vascular defects in the yolk sac (van Meeteren *et al*, 2006; Koike *et al*, 2009). Moreover, catalytic site-mutated *atx* knock-in mice are also embryonic lethal due to severe vascular defects (Ferry *et al*, 2007), suggesting that ATX-LPA signaling plays a fundamental role during vascular development. Recently, LPA was reported to regulate definitive erythropoiesis through activating LPAR3 in a human hematopoietic

1 State Key Laboratory of Cell Biology, Institute of Biochemistry and Cell biology, Shanghai Institutes for Biological Sciences, Graduate School of the Chinese Academy of Sciences, Chinese Academy of Sciences, Shanghai, China
2 Howard Hughes Medical Institute, Children's Medical Center Research Institute, Department of Pediatrics, University of Texas Southwestern Medical Center, Dallas, TX, USA
3 Center for Bioinformatics, State Key Laboratory of Protein and Plant Gene Research, College of Life Sciences, Peking University, Beijing, China
4 Institute of Neuroscience and State Key Laboratory of Neuroscience, Shanghai Institutes for Biological Sciences, Chinese Academy of Sciences, Shanghai, China
5 Shanghai Key Laboratory of Signaling and Disease Research, School of Life Science and Technology, Tongji University, Shanghai, China
†These authors contributed equally to this work
*Corresponding author. Tel: +86 21 54921371; Fax: +86 21 54921011; E-mails: gpei@sibs.ac.cn; peigang@tongji.edu.cn

stem cell differentiation model (Chiang *et al*, 2011); however, whether LPA signaling also regulates primitive hematopoiesis during early development remains unclear.

In this study, we identified LPA as a critical regulator of hemangioblast formation and primitive hematopoiesis by analyzing the hematopoietic differentiation of mESCs and the zebrafish embryogenesis. Furthermore, we showed that LPAR1, but not LPAR3, mediates this effect by activating PI3K/Akt-Smad pathway, highlighting the role of LPA as a nutrient-derived developmental cue during early development.

Results

LPA regulates hematopoietic differentiation

Previously, we had successfully identified F2r as a critical regulator of hematopoiesis through a microarray analysis (Hailesellasse Sene *et al*, 2007; Yue *et al*, 2012). In addition to *F2r*, we also found that *lpar1* and *lpar3* were significantly up-regulated during *in vitro* hematopoietic differentiation of mESCs (Supplementary Fig S1A and B). Interestingly, *atx* expression peaked at day 4 of EB formation before *lpar1* and *lpar3* (Supplementary Fig S1C), which coincided with the reported window of hemangioblast formation and blood fate specification (between day 3 and day 4 of hematopoietic differentiation) (Kennedy *et al*, 1997), indicating that ATX-LPA signaling may play a role during hematopoietic differentiation.

Next, we used both pharmacological and genetic approaches to modulate LPA signaling during hematopoietic differentiation. Treatment of two structurally different LPAR1/3-specific antagonists, Ki16425 and VPC32183, dose-dependently reduced $CD41^+$ hematopoietic cell percentage in day 6 EBs (Fig 1A–B and Supplementary Fig S2A–B). Consistently, quantitative real-time PCR (qPCR) analyses showed that hematopoietic transcription factors *gata1, scl, runx1, cmyb* as well as, *beta-h1* and *beta-major* hemoglobins were all down-regulated after LPAR1/3 antagonist treatment (Fig 1C and Supplementary Fig S2C). Methylcellulose colony-forming cell assay (M3434) showed that LPAR1/3 antagonism significantly reduced the primitive erythroid colony numbers (Ery-P) (Fig 1D and Supplementary Fig S2D), as well as the definitive erythroid (cfu-E) and granulocyte/monocyte (cfu-G/M/GM) colony numbers (Fig 1E and Supplementary Fig S2E). To rule out the possibility that the inhibition of hematopoietic differentiation was caused by increased apoptosis, day 6 EBs were dissociated and stained with Annexin-V and PI. Flow cytometry analyses revealed that LPAR1/3 antagonism did not significantly change the percentage of cells that are undergoing apoptosis (Supplementary Fig S3A–D). Finally, we explored the role of ATX during hematopoietic differentiation by using the ATX inhibitor HA130 in a serum-free differentiation medium (Gadue *et al*, 2006), since serum contains high levels of LPA. HA130 significantly inhibited $CD41^+$ cell percentage in a dose-dependent manner (Fig 1F) and down-regulated the expression of hematopoietic markers (Fig 1G). In addition, HA130 also notably reduced the Ery-p (Fig 1H), cfu-E, and cfu-G/M/GM colony numbers (Fig 1I).

Since Ki16425 and VPC32183 block both LPAR1 and LPAR3, we further attempted to clarify the downstream receptor by using small interference RNA (siRNA)-mediated knockdown. Stable mESC lines harboring *Lpar1* and/or *Lpar3* siRNAs were constructed using lentivirus infection followed by flow cytometry sorting. The knockdown efficiency was determined by qPCR (Fig 2A). Genetic inhibition of *lpar1* significantly decreased $CD41^+$ cell percentage (Fig 2B), hematopoietic marker expression (Fig 2C), and colony-forming cell numbers (Fig 2D and E). In contrast, inhibition of *lpar3* showed no significant changes, and simultaneous knockdown of *lpar1* and *lpar3* demonstrated no synergistic effects compared to *lpar1* knockdown (Fig 2B–E). We also established a mESC line stably expressing the *Atx* siRNA and differentiated it in a serum-free medium (Fig 2F). Consistently, knockdown of *atx* also significantly reduced $CD41^+$ cell percentage, hematopoietic marker expression, and the colony-forming cell numbers (Fig 2G–J). These results not only confirmed the pharmacological blockage data, but also indicated that LPAR1 mediates the downstream effects of LPA to regulate hematopoietic differentiation.

To determine whether LPA is sufficient to promote hematopoietic differentiation, we utilized a serum-free system to minimize the effect of serum-derived LPA (Chiang *et al*, 2011). LPA significantly increased $CD41^+$ cell percentage and hematopoietic marker expression (Supplementary Fig S4A–C), which was abolished by Ki16425 or VPC32183 treatment (Supplementary Fig S4D). Similarly, the effect of LPA was also abolished after *lpar1* knockdown (Supplementary Fig S4E), indicating that LPA promotes hematopoietic differentiation via LPAR1. In contrast, treatment of sphingosine-1-phosphate (S1P), another prototypical lysophospholipid, or S1P receptor agonist FTY720P, did not affect $CD41^+$ cell percentage (Supplementary Fig S5A and B). Taken together, these data provide evidence that LPA regulates hematopoietic differentiation *in vitro*.

LPA regulates hemangioblast formation

During *in vitro* hematopoietic differentiation, mESCs first generate $flk1^+$ hemangioblasts, which then give rise to $CD41^+$ hematopoietic

Figure 1. Pharmacological blockage of ATX-LPA signaling inhibits hematopoietic differentiation.

A Representative flow cytometry data for CD41 staining in day 6 EBs, treated with DMSO or 30 μM Ki16425 from day 2 to day 6.

B Dose effect of Ki16425 on mESC hematopoietic differentiation. The relative fold changes of $CD41^+$ cell percentage were shown ($n = 5$).

C qPCR analyses of hematopoietic marker expressions ($n = 4$).

D, E Methylcellulose colony-forming cell assay (M3434). Primitive erythroid colonies were scored 6 days after culture in M3434 (D) ($n = 4$). Definitive colonies were scored 10 days after culture in M3434 (E) ($n = 4$). Insets show average distribution of hematopoietic colonies. Ery-P: primitive erythroid; cfu-E: definitive erythroid; cfu-G/M/GM: granulocytes/macrophages/granulocyte macrophages; cfu-GEMM: granulocyte/erythroid/myeloid megakaryocytes.

F Dose effect of HA130 on $CD41^+$ cell percentage ($n = 3$).

G qPCR analyses of hematopoietic marker expressions ($n = 4$).

H, I Methylcellulose colony-forming cell assay (M3434). Primitive (H) and definitive (I) colonies were cultured and scored as in (D) and (E) ($n = 3$ per group).

Data information: Data shown are means ± s.e.m., $*P < 0.05$, $**P < 0.01$, $***P < 0.001$ versus the corresponding control.

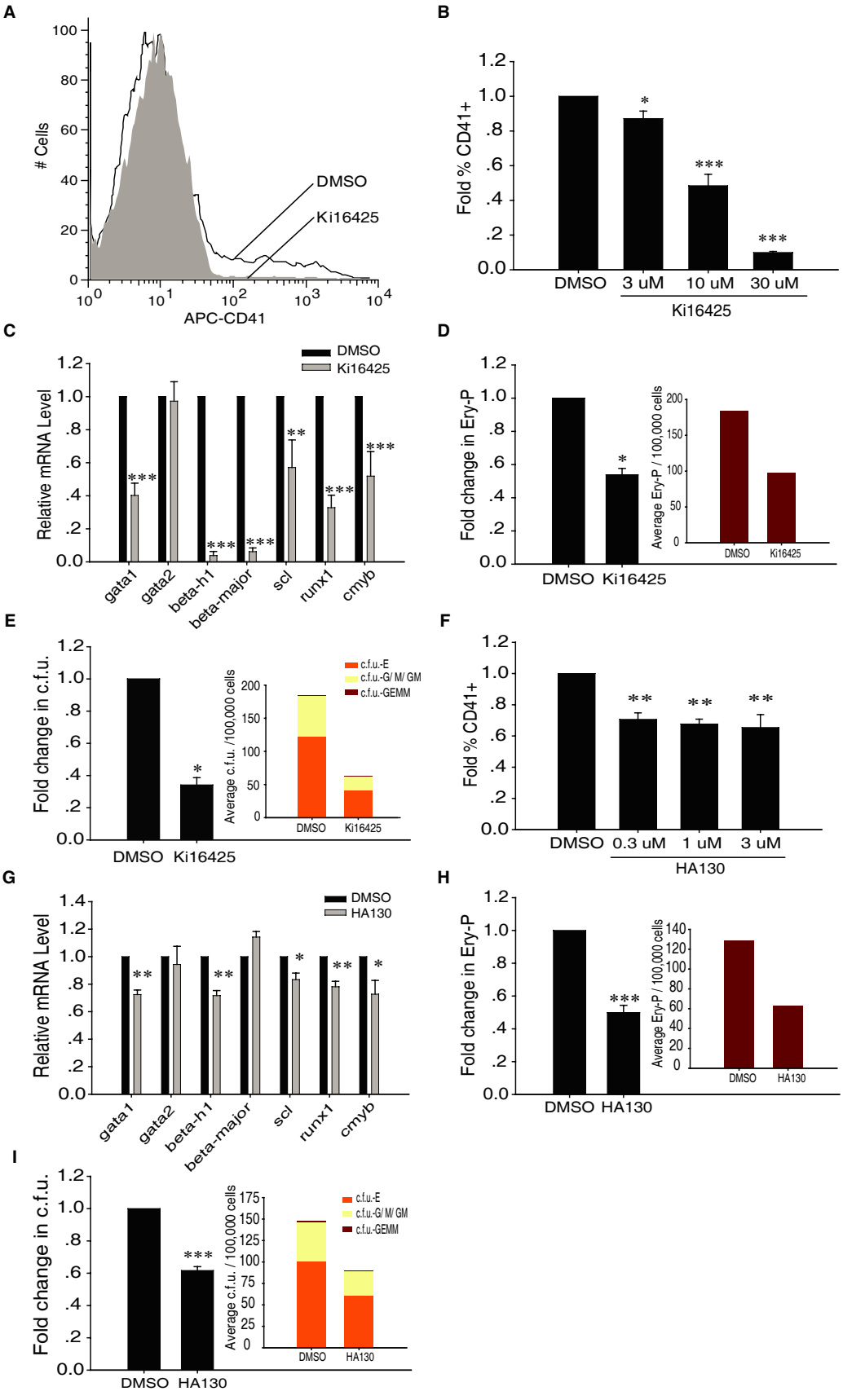
A
Cells
APC-CD41
DMSO
Ki16425
B
Fold % CD41+
DMSO
3 uM
10 uM
30 uM
Ki16425
C
Relative mRNA Level
DMSO
Ki16425
gata1
gata2
beta-h1
beta-major
scl
runx1
cmyb
D
Fold change in Ery-P
Average Ery-P / 100,000 cells
DMSO
Ki16425
E
Fold change in c.f.u.
Average c.f.u. /100,000 cells
c.f.u.-E
c.f.u.-G/ M/ GM
c.f.u.-GEMM
F
Fold % CD41+
DMSO
0.3 uM
1 uM
3 uM
HA130
G
Relative mRNA Level
HA130
H
Fold change in Ery-P
I
Fold change in c.f.u.

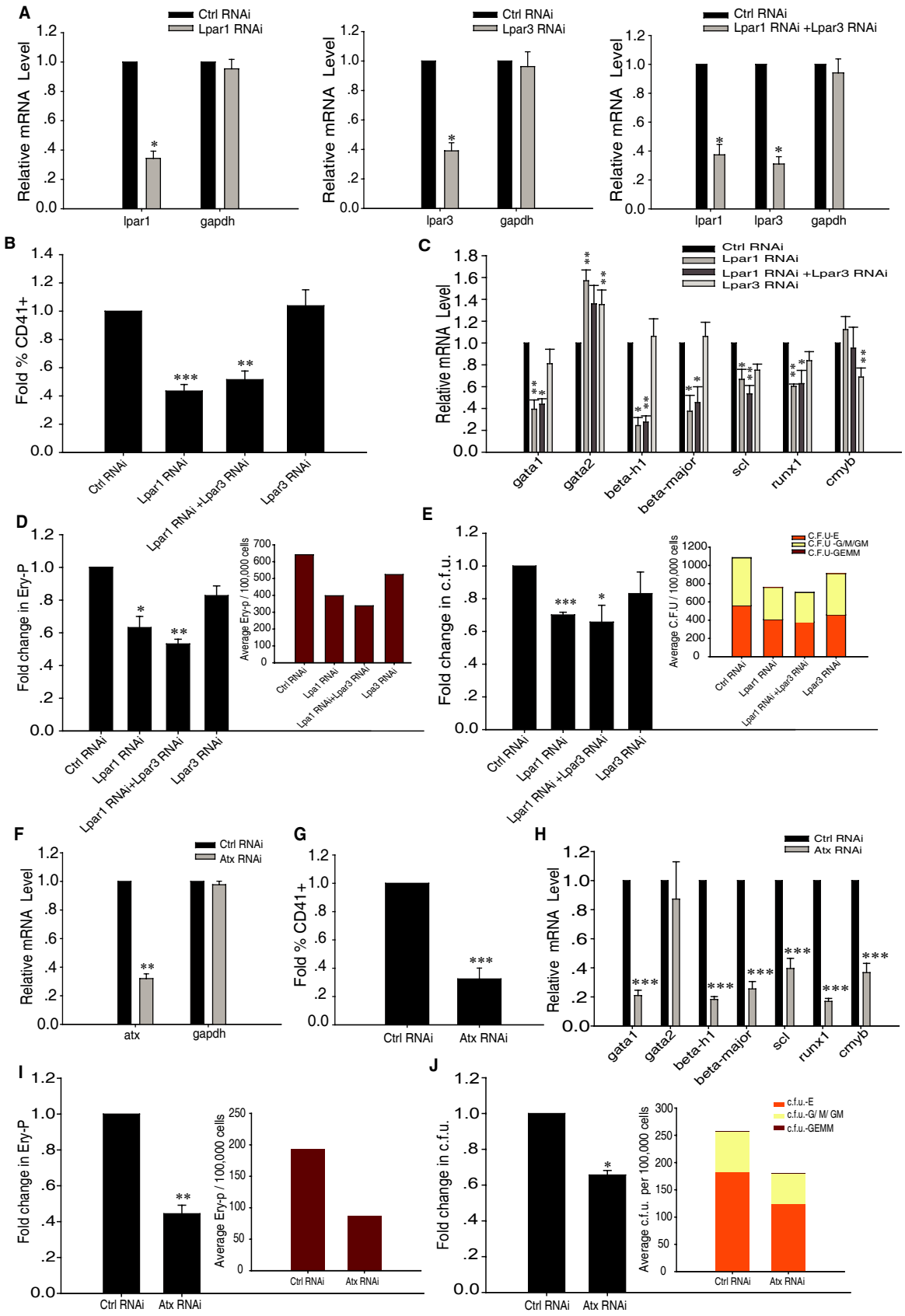

progenitor cells and more mature hematopoietic cell types (Eilken *et al*, 2009; Lancrin *et al*, 2009). Thus, we went on to determine whether LPA signaling regulates hemangioblast formation. Ki16425 and VPC32183 treatment significantly reduced flk1$^+$ cell percentage in day 4 EBs (Fig 3A–B and Supplementary Fig S2F–G). Consistently, qPCR analyses showed that LPAR1/3 antagonism notably inhibited the expression of *flk1* as well as other hematopoietic transcription factors. In contrast, the endoderm marker *lamb1*, panmesoderm marker *brachyury*, and ectoderm marker *beta-tub3* were not affected, suggesting that the specification of three germ layers was not generally affected (Fig 3C and Supplementary Fig S2H). In addition, we performed blast colony-forming cell (BL-CFC) assay to functionally measure hemangioblast numbers and found that LPAR1/3 antagonism led to significantly reduced BL-CFCs (Fig 3D and Supplementary Fig S2I). The inhibitory effect of LPAR1/3 antagonism on hemangioblast formation was not a consequence of increased cell apoptosis (Supplementary Fig S3E–H). Similarly, ATX inhibitor HA130 also significantly impaired hemangioblast formation in day 4 EBs (Fig 3E–G).

Consistent with the pharmacological results, siRNA-mediated knockdown of *lpar1* dramatically reduced flk1$^+$ cell percentage, *flk1* and hematopoietic marker expression, and the BL-CFC numbers in day 4 EBs, whereas knockdown of *lpar3* did not show any inhibitory effects (Fig 4A–C). The fact that LPAR3 had no effects in regulating hematopoiesis *in vitro* is probably due to the late onset of *lpar3* expression during EB differentiation (Supplementary Fig S1B). Similarly, knockdown of *atx* also significantly compromised hemangioblast formation (Fig 4D–F). Furthermore, high concentrations of LPA (10–30 μM) significantly increased flk1$^+$ cell percentage in the serum-free system (Supplementary Fig S6A), whereas treatment of S1P or FTY720P did not affect flk1$^+$ cell percentage (Supplementary Fig S6B and C). Collectively, these results showed that LPA signaling is both required and sufficient for hemangioblast formation.

ATX-LPA signaling regulates hematopoietic differentiation through PI3K/Akt-Smad pathway

Next, we attempted to illustrate the downstream mechanisms of LPA signaling during hematopoietic differentiation. To test whether there is cross talk between LPA signaling and known hematopoietic pathways, we applied the inhibitors of several hematopoietic pathways in combination with LPA in a serum-free differentiation system and analyzed CD41$^+$ hematopoietic cell percentage. BMP pathway inhibitor dorsomorphin significantly inhibited hematopoietic differentiation, which was consistent with the fact that BMP signal is critical for mesoderm induction (Soderberg *et al*, 2009). In contrast, inhibition of FGF pathway, Hedgehog pathway, or nitric oxide pathway did not notably abolish the effects of LPA (Supplementary Fig S8A). Dorsomorphin was previously shown to inhibit VEGF receptor 2 (Flk1) signaling (Hao *et al*, 2010); however, VEGF receptor inhibitor axitinib did not abolish the effect of LPA treatment (Supplementary Fig S8B), suggesting that there is no cross talk between LPA signaling and Flk1 signaling. LPA was also shown to activate β-catenin, a key downstream component of Wnt signaling pathway, during definitive erythropoiesis (Chiang *et al*, 2011). However, β-catenin inhibitor quercetin also did not abolish the effect of LPA (Supplementary Fig S8C), indicating that LPA signaling and Wnt pathway do not cross talk during hematopoietic differentiation.

After stimulation by LPA, LPAR1 binds to G proteins such as G_i, G_q, and $G_{12/13}$, which further activates PI3K/Akt, PKC, or RhoA/Rock pathway, respectively (Fukushima *et al*, 1998, 2001; Contos *et al*, 2000). Interestingly, Gi inhibitor PTX significantly abolished the effect of LPA, whereas ROCK, Rac1, and PKC inhibitors did not affect LPA signaling (Fig 5A and Supplementary Fig S8D). The effect of LPA was also abolished by PI3K inhibitors LY294002, wortmannin, and Akt inhibitor AKT VIII (Fig 5B). Consistently, Western blot analysis showed that *lpar1*, but not *lpar3*, knockdown led to decreased Akt phosphorylation in day 4 EBs, while simultaneous knockdown of both *lpar1* and *lpar3* had no synergistic effects (Fig 5C).

Previous studies demonstrated that Smad1 stimulates hemangioblast formation as well as hematopoietic development (Zafonte *et al*, 2007; Cook *et al*, 2011; Zhang *et al*, 2011). Since Akt was known to positively regulate Smad1 phosphorylation (Jin *et al*, 2011), we hypothesized that Smad1 may function as the downstream mediator of ATX-LPA signaling. Indeed, knockdown of *lpar1*, but not *lpar3*, significantly decreased Smad1 phosphorylation (Fig 5D). Importantly, LPA significantly increased Akt phosphorylation and Smad1 phosphorylation, which could be abolished by PI3K inhibitor or Akt inhibitor, while Erk1/2 phosphorylation was not affected (Fig 5E). In contrast, LPAR1 antagonist Ki16425 significantly decreased Akt and Smad1 phosphorylation, but not Erk1/2 phosphorylation, while over-expressing the constitutively active form of AKT (CA-AKT) led to opposite effects and partially rescued the inhibitory effects of Ki16425 on Smad1 phosphorylation (Fig 5F). Taken together, these data demonstrated that PI3K/Akt-Smad pathway mediates LPA signaling during hematopoietic differentiation.

Figure 2. Genetic blockage of ATX–LPA signaling inhibits hematopoietic differentiation.

A qPCR analyses of *lpar1* or *lpar3* knockdown efficiency (n = 4 per group).
B Flow cytometry analyses of CD41$^+$ cell percentage. The relative fold changes of CD41$^+$ cell percentage were shown (n = 4).
C qPCR analyses of hematopoietic markers (n = 5).
D, E Methylcellulose colony-forming cell assay (M3434). Primitive erythroid colonies were scored 6 days after culture in M3434 (D) (n = 4). Definitive colonies were scored 10 days after culture in M3434 (E) (n = 4). Insets show average distribution of hematopoietic colonies.
F qPCR analyses of *atx* knockdown efficiency (n = 3). expressions in whole EBs of day 6 (n = 4).
G Effect of *atx* knockdown on CD41$^+$ cell percentage (n = 6).
H qPCR analyses of hematopoietic marker expressions in day 6 whole EBs (n = 4).
I, J Methylcellulose colony-forming cell assay (M3434). Primitive (I) and definitive (J) colonies were cultured and scored as in (D) and (E) (n = 4 per group).

Data information: Data shown are means ± s.e.m., *P < 0.05, **P < 0.01, ***P < 0.001 versus the corresponding control.

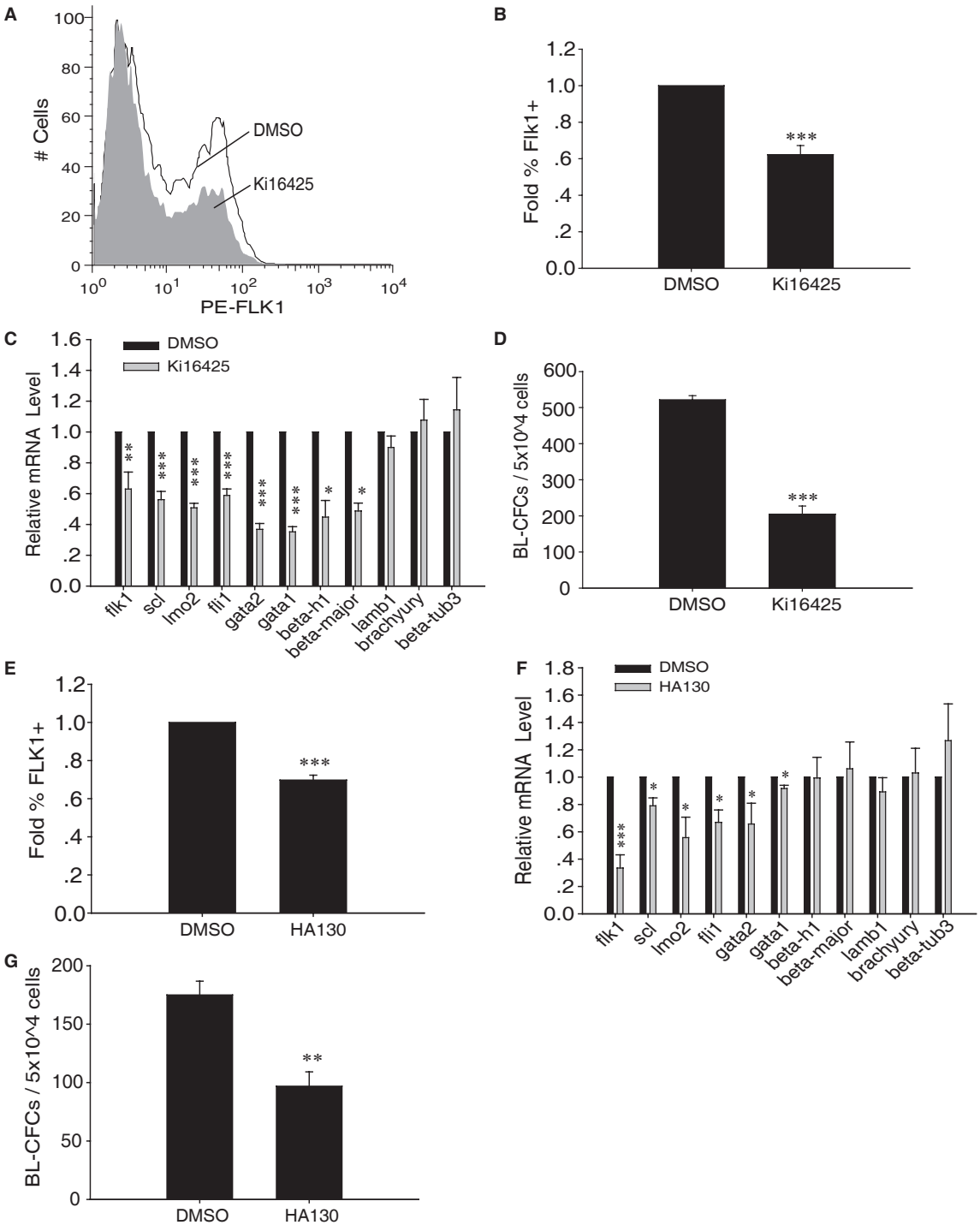

Figure 3. Pharmacological blockage of ATX-LPA signaling inhibits hemangioblast formation.

A Representative flow cytometry data for Flk1 staining in day 4 whole EBs. EBs were treated with DMSO or 30 μM Ki16425 from day 2 to day 4 and analyzed by flow cytometry.

B Effect of Ki16425 treatment on Flk1$^+$ cell percentage (n = 5).

C qPCR analyses of hematopoietic and germ layer marker expressions (n = 4). Endoderm marker: *lamb1*; mesoderm marker: *brachyury*; ectoderm marker: *beta-tub3*.

D BL-CFC assay. Day 4 EBs treated as in (A) were digested with trypsin and cultured in BL-CFC medium. Blast colonies were identified and scored by their distinctive morphology 4 days later (n = 4).

E Effect of HA130 on Flk1$^+$ cell percentage (n = 4).

F qPCR analyses of hematopoietic and germ layer marker expressions (n = 3).

G BL-CFC assay (n = 3). Blast colonies were cultured and scored as in (D).

Data information: Data shown are means ± s.e.m., *P < 0.05, **P < 0.01, ***P < 0.001 versus the corresponding control.

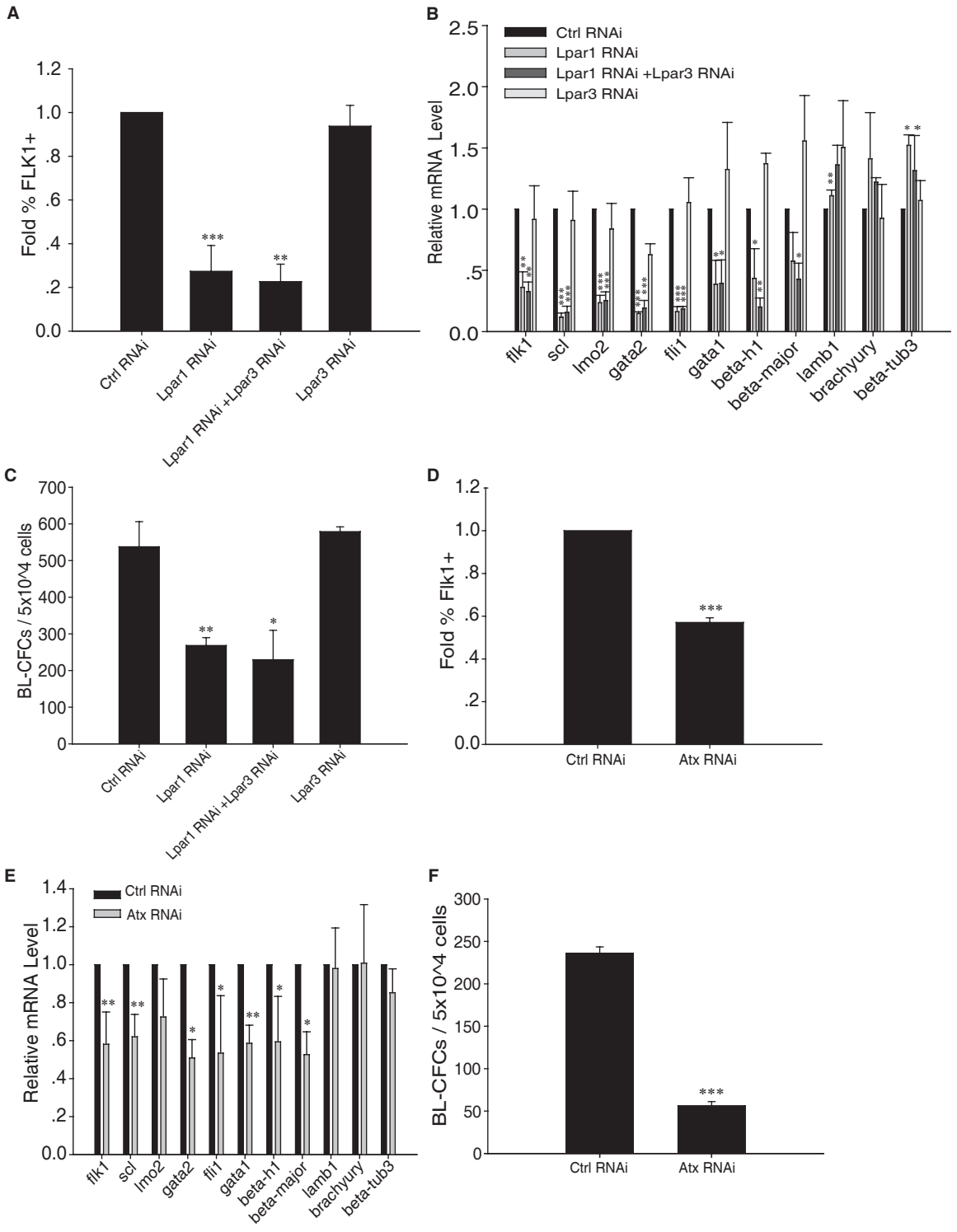

Figure 4. Genetic blockage of ATX-LPA signaling inhibits hemangioblast formation.

A Effects of *lpar1* and/or *lpar3* knockdown on Flk1$^+$ cell percentage in day 4 whole EBs (n = 4).

B qPCR analyses of hematopoietic and germ layer marker expressions (n = 4).

C BL-CFC assay. Day 4 EBs were digested with trypsin and cultured in BL-CFC medium. Blast colonies were identified and scored 4 days later (n = 3).

D Effect of *atx* knockdown on Flk1$^+$ cell percentage (n = 3).

E qPCR analyses of hematopoietic and germ layer marker expressions (n = 4).

F BL-CFC assay (n = 4). Blast colonies were cultured and scored as in (C).

Data information: Data shown are means ± s.e.m., *P < 0.05, **P < 0.01, ***P < 0.001 versus the corresponding control.

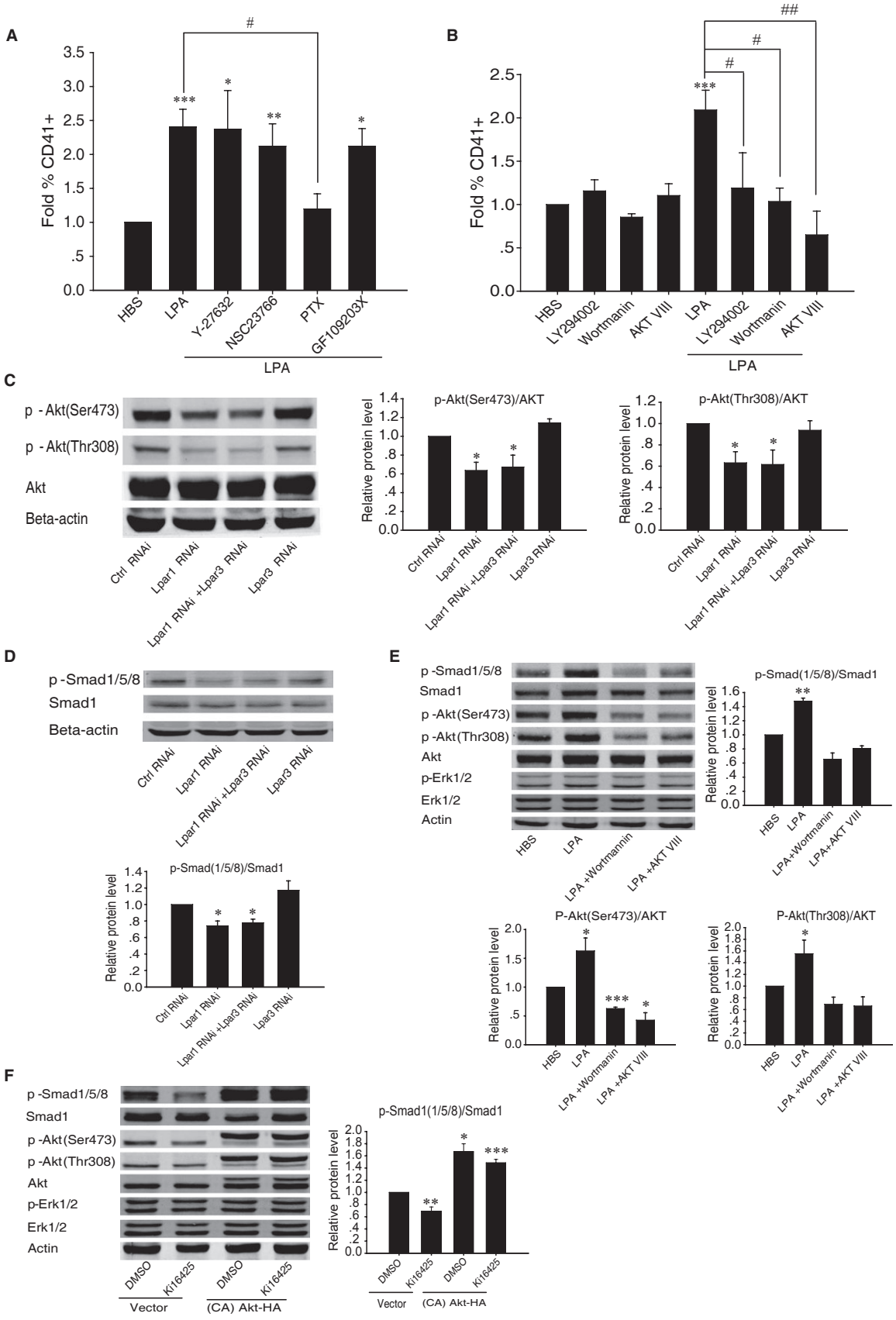

Figure 5. ATX–LPA signaling regulates hematopoietic differentiation through PI3K/Akt-Smad pathway.

A, B Flow cytometry analyses of $CD41^+$ cell percentage. EBs were treated with 100 nM LPA alone, or together with ROCK inhibitor Y-27632 (10 μM), Rac1 inhibitor NSC23766 (100 μM), Gi inhibitor PTX (80 ng/ml), or PKC inhibitor GF109203X (1 μM) from EB day 2 to day 6 in serum-free culture (A) (n = 3). EBs were treated with 100 nM LPA alone, or together with PI3K inhibitor LY294002 (4 μM), wortmannin (3 μM) or AKT inhibitor AKT VIII (2 μM) from EB day 2 to day 6 in serum-free culture (B) (n = 3).

C, D Western blot analyses. Day 4 EBs, stably expressing *Lpar1* or *Lpar3* siRNA, were digested with trypsin, and protein samples were prepared. Beta-actin was used as the loading control. The quantification results were plotted as ratio between phosphorylated Akt and total AKT after normalization to beta-actin levels (C) (n = 3). The quantification result of phosphorylated Smad1/5/8 was plotted as ratio between phosphorylated Smad1/5/8 and total Smad1 after normalization to beta-actin levels (D) (n = 4).

E, F Epistatic analyses. EBs were treated with LPA alone, or together with PI3K inhibitor wortmannin (3 μM) or AKT inhibitor AKT VIII (2 μM) from EB day 2 to day 4 in serum-free culture. Day 4 EBs were digested with trypsin, and protein samples were prepared. Beta-actin was used as the loading control (E) (n = 3). mESCs stably expressing vector or CA-Akt were differentiated as EBs and treated with DMSO or 10 μM Ki6425 from day 2 to day 4 (F) (n = 3). Beta-actin was used as the loading control.

Data information: Data shown are means ± s.e.m., $*P < 0.05$, $**P < 0.01$, $***P < 0.001$ versus the corresponding control.

ATX-LPA signaling regulates primitive hematopoiesis during zebrafish embryogenesis

To explore the effect of ATX-LPA signaling on hematopoiesis *in vivo*, we detected the expression changes of *lpar1*, *lpar3*, and *atx* during zebrafish embryogenesis by qPCR analysis. *Lpar1* was markedly up-regulated from 12 hours post-fertilization (hpf) (Supplementary Fig S1D), whereas *lpar3* first peaked at 6 hpf and then gradually increased after 24 hpf (Supplementary Fig S1E), which was identical to the previously reported pattern of zebrafish *lpar3* (Lai *et al*, 2012). *Atx w*as dramatically up-regulated after 12 hpf (Supplementary Fig S1F).

Next, we used both pharmacological and genetic approaches to test the role of ATX-LPA signaling during zebrafish hematopoiesis. Whole mount *in situ* hybridization (WISH) analyses showed that Ki16425 treatment dramatically decreased the expression of hemangioblast markers *lmo2* and *scl* in the lateral-ventral mesoderm at 12 hpf (Fig 6A, n = 28/29; Fig 6B, n = 17/19; Fig 6C, n = 16/21; Fig 6D, n = 17/26). Consistently, Ki16425 also decreased the expression of primitive hematopoietic markers *gata1* and *scl* in the intermediate cell mass (ICM) at 24 hpf (Fig 6E, n = 16/19; Fig 6F, n = 17/20; Fig 6G, n = 20/30; Fig 6H, n = 19/26), as well as primitive myeloid markers *l-plastin* and *mpo* at 26 hpf (Supplementary Fig S11A, n = 13/14; Supplementary Fig S11B, n = 18/19; Supplementary Fig S11C, n = 20/27; Supplementary Fig S11D, n = 19/23). Recently, RAGE (receptor for advanced glycation end products) was shown to be a non-GPCR receptor for LPA (Rai *et al*, 2012). However, RAGE antagonist FPS-ZM1 did not affect hematopoietic development (Supplementary Fig S10A, n = 21/26; Supplementary Fig S10B, n = 20/28; Supplementary Fig S10C, n = 14/19; Supplementary Fig S10D, n = 15/18; Supplementary Fig S10E, n = 31/34; Supplementary Fig S10F, n = 32/35; Supplementary Fig S10G, n = 28/35; Supplementary Fig S10H, n = 17/22).

In addition, we also injected the morpholino antisense oligonucleotides (MOs) at one-cell stage to block ATX-LPA pathway at the translational level. The specificity of *Lpar1* MO was confirmed by a reporter assay (Supplementary Fig S9A–D). 6 ng *Lpar1* MO injection remarkably decreased the expression of hemangioblast markers *lmo2* and *scl* at 12 hpf (Fig 6I, n = 48/53; Fig 6J, n = 31/35; Fig 6L, n = 56/67; Fig 6M, n = 39/50), ICM markers *gata1* and *scl* at 24 hpf (Fig 6O, n = 51/56; Fig 6P, n = 31/36; Fig 6R, n = 43/52; Fig 6S, n = 42/46) and primitive myeloid markers *l-plastin* and *mpo* at 26 hpf (Supplementary Fig S11E, n = 52/60; Supplementary Fig S11F, n = 53/66; Supplementary Fig S11H, n = 42/50; Supplementary Fig S11I, n = 36/45). Importantly, these defects could be largely restored by co-injection of *lpar*1 mRNA (Supplementary Fig S12C, n = 47/48; Supplementary Fig S12F, n = 34/37; Supplementary Fig S12I, n = 28/30; Supplementary Fig S12L, n = 34/39; Supplementary Fig S12O, n = 19/23; Supplementary Fig S12R, n = 39/42). In contrast, 2.5 ng *Lpar3* MO injection (Chiang *et al*, 2011) had no such inhibitory effects (Fig 6K, n = 30/34; Fig 6N, n = 37/43; Fig 6Q, n = 51/58; Fig 6T, n = 48/55; Supplementary Fig S11G, n = 22/31; Supplementary Fig S11J, n = 34/45). Increasing the *Lpar3* MO dose up to 5 ng caused developmental delay and reduced the expression of hemangioblast markers *lmo2* and *scl* at 12 hpf (Supplementary Fig S10I, n = 64/65; Supplementary Fig S10J, n = 32/35; Supplementary Fig S10K, n = 37/39; Supplementary Fig S10L, n = 22/28), but did not alter the expression of ICM markers *gata1* and *scl* at 24 hpf (Supplementary Fig S11M, n = 27/27; Supplementary Fig S11N, n = 29/29; Supplementary Fig S11O, n = 36/36; Supplementary Fig S11P, n = 31/32). Importantly, 0.5 ng *Atx* MO injection also decreased the expression of *lmo2* and *scl* at 12 hpf (Fig 6U, n = 22/38; Fig 6V, n = 26/29; Fig 6W, n = 18/26; Fig 6X, n = 20/23), *gata1*, and *scl* at 24 hpf (Fig 6Yi, n = 30/44; Fig 6Yii, n = 17/26; Fig 6Zi, n = 23/34; Fig 6Zii, n = 15/19), as well as *l-plastin* and *mpo* at 26 hpf (Supplementary Fig S11K, n = 59/66; Supplementary Fig S11L, n = 53/61; Supplementary Fig S11M, n = 15/17; Supplementary Fig S11N, n = 12/14). The specificity of *Atx* MO was verified (Supplementary Fig S9E–H). Collectively, these results suggested that ATX-LPA signaling is necessary for hemangioblast formation and primitive hematopoiesis *in vivo*.

Discussion

Hematopoietic development is controlled by the concerted actions of both intrinsic transcription factors, as well as extracellular signals generated by the local environment. In this study, we found that ATX-LPA signaling functions as an evolutionarily conserved pathway that is critically involved in hemangioblast formation and primitive hematopoiesis. Since LPA is a classical metabolite of PC, a major nutrient in the early hematopoietic microenvironment, our results unraveled the morphogenic role of early nutrients and a GPCR-mediated extracellular regulatory mechanism of hemangioblast formation.

Lysophospholipids, including LPA and S1P, have been previously implicated in cardiovascular development (Birgbauer & Chun, 2006). S1P regulates cardiac differentiation of mouse ES cells and vascular maturation in mouse (Liu *et al*, 2000; Allende *et al*, 2003; Sachinidis *et al*, 2003). In addition, S1P and LPA are also shown to be critical for vascular development and stabilization in zebrafish (Yukiura *et al*, 2011; Gaengel *et al*, 2012; Lai *et al*, 2012). Interestingly, 0.5 ng *Atx* MO injection decreased the expression of endothelial markers *fli-1* and *flk1* in the intersegmental vessel (ISV) (Supplementary Fig S13A, $n = 29/32$; Supplementary Fig S13B, $n = 22/28$; Supplementary Fig S13C, $n = 13/13$; Supplementary Fig S13D, $n = 12/14$) at 22 hpf, while higher doses of *Atx* MO led to embryonic lethality and completely abolished the hemangioblast markers (Unpublished observations), further indicating that ATX regulates hemangioblast specification. The discrepancy between our results and a previous study that *Atx* morphants had only defects in segmental artery sprouting (Yukiura *et al*, 2011) is possibly due to the fact that we use different sequences of *Atx* MO. Furthermore, our observations are consistent with the lethal phenotype of *atx*-deficient mice that were associated with vascular defects in the yolk sac (van Meeteren *et al*, 2006; Koike *et al*, 2009). Since hemangioblast is the common progenitor giving rise to both hematopoietic and endothelial lineages, our results suggested that LPA participates in both vascular and hematopoietic development through hemangioblast regulation. Future studies are needed to carefully examine whether there are hemangioblast defects associated with *atx* or *lpar1* knockout mice during embryonic development.

LPA can be generated both intracellularly by cytosolic phospholipase A2 (cPLA2) and extracellularly by sPLA2 or ATX (Mills & Moolenaar, 2003). In contrast to ATX, cPLA2 and sPLA2 generate LPA by hydrolyzing phosphatidic acid (PA). The intracellular LPA may not play an important role during hematopoietic differentiation, since inhibition of ATX or LPAR1 only affects the extracellular LPA signaling. Consistently, cPLA2 inhibitor OBAA did not affect hematopoietic differentiation (Supplementary Figs S5C and S7A). Similarly, sPLA2 inhibitor BPB also did not affect hematopoietic differentiation (Supplementary Figs S5D and S7B), indicating that the PC/LPC/LPA, but not PA/LPA, metabolic pathway is the main source of LPA production during hematopoiesis. Although previous studies show that PC can be released from cell membrane during apoptosis (Chaurio *et al*, 2009; Schmitz & Ruebsaamen, 2009), we found that the caspase inhibitor did not affect hematopoietic differentiation (Supplementary Figs S5E and S7C), suggesting that apoptotic cell membrane is not the main source of PC.

The transient nature of hemangioblast *in vivo* makes it particularly challenging to define its underlying regulatory mechanisms. Thus, the embryonic stem cell differentiation system has been used to study hemangioblast *in vitro* (Kennedy *et al*, 1997; Park *et al*, 2005). The BMP4 signaling is well known to be required for hemangioblast formation (Johansson & Wiles, 1995; Winnier *et al*, 1995; Park *et al*, 2004; Nostro *et al*, 2008). BMP4 stimulation activates the phosphorylation of Smad1/5/8, which then translocates to the nucleus to initiate downstream transcription (Feng & Derynck, 2005; Soderberg *et al*, 2009). Here, we showed that LPA signaling activates PI3K/Akt pathway to promote the phosphorylation of Smad1/5/8 and that LPA and BMP4 have synergistic effects in promoting hematopoietic differentiation (Supplementary Fig S4F). Consistently, LPAR1 antagonist VPC32183 significantly reduced Smad1 phosphorylation in the presence or absence of BMP4 (Supplementary Fig S8E). In addition, BMP pathway inhibitor dramatically decreased Smad1 phosphorylation without affecting AKT phosphorylation and abolished the effect of LPA (Supplementary Fig S8F). These data highlighted the role of Smad in the cross talk between LPA and BMP4 signaling.

In summary, our study demonstrates that nutrient-derived LPA signaling specifies hematopoietic development through hemangioblast regulation and shed light on the pivotal role of GPCR and lipid metabolism during early development. Interestingly, insufficient or excessive nutrition during pregnancy was shown to increase the risk of metabolic syndromes in the adulthood (Guo & Jen, 1995; Hales & Barker, 2001; Khan *et al*, 2005). Thus, it is intriguing to examine whether altered metabolism of yolk sac lipids contributes to the later development of adult metabolic or hematopoietic diseases in the future.

Materials and Methods

ES cell culture and differentiation

E14.1 mouse ES cells were cultured and differentiated as previously described (McKinney-Freeman *et al*, 2008). Briefly, undifferentiated mESCs were maintained in pre-differentiation medium 2 days before hematopoietic differentiation [15% FBS, 1 mM sodium pyruvate (Sigma), 2 mM glutamine (Invitrogen), 0.1 mM non-essential amino acid (Merck Millipore), 10 ng/ml LIF, 100 μM monothioglycerol (Sigma) with 100 U/ml penicillin and 100 μg/ml streptomycin in IMDM (Sigma)]. To form hematopoietic EBs, mESCs were trypsinized into single cells, diluted at 100 mESCs/15 μl differentiation medium [200 μg/ml holo-transferrin (Calbiochem), 4.5 mM monothioglycerol, 15% FBS, 0.5 mM ascorbic acid (Sigma), 2 mM glutamine with 100 U/ml penicillin and 100 μg/ml streptomycin in IMDM], and inverted cultured for 2 days. EBs were then collected and cultured with rotation in 35 mm Petri dishes. Fresh differentiation medium was changed every 2 days. The serum-free differentiation

Figure 6. ATX–LPA signaling is required for hemangioblast formation and primitive hematopoiesis in zebrafish.

A–H WISH analyses for embryos treated with Ki16425. Zebrafish embryos treated with DMSO or 30 μM Ki16425 were hybridized with riboprobes to hemangioblast markers *lmo2* (A and B) and *scl* (C and D) at 12 hpf, or with riboprobes to primitive hematopoietic markers *gata1* (E and F) and *scl* (G and H) at 24 hpf. Embryos were dorsal views with anterior to the top (A–D), or lateral views with anterior to the left (E–H).

I–T WISH analyses for embryos injected with *Lpar1* or *Lpar3* MO. Zebrafish embryos injected with 4 ng Ctrl MO, 6 ng *Lpar1* MO, or 2.5 ng *Lpar3* MO at one-cell stage were hybridized with riboprobes to hemangioblast markers *lmo2* (I–K) and *scl* (L–N) at 12 hpf, or with riboprobes to primitive hematopoietic markers *gata1* (O–Q) and *scl* (R–T) at 24 hpf. Embryos were dorsal views with anterior to the top (I–N) or lateral views with anterior to the left (O–T).

U–Zii WISH analyses for embryos injected with *Atx* MO. Zebrafish embryos injected with 0.5 ng Ctrl MO or 0.5 ng *Atx* MO at one-cell stage were hybridized with riboprobes to hemangioblast markers *lmo2* (U and V) and *scl* (W and X) at 12 hpf, or with riboprobes to primitive hematopoietic markers *gata1* (Yi and Yii) and *scl* (Zi and Zii) at 24 hpf. Embryos were dorsal views with anterior to the top (U–X) or lateral views with anterior to the left (Yi–Zii).

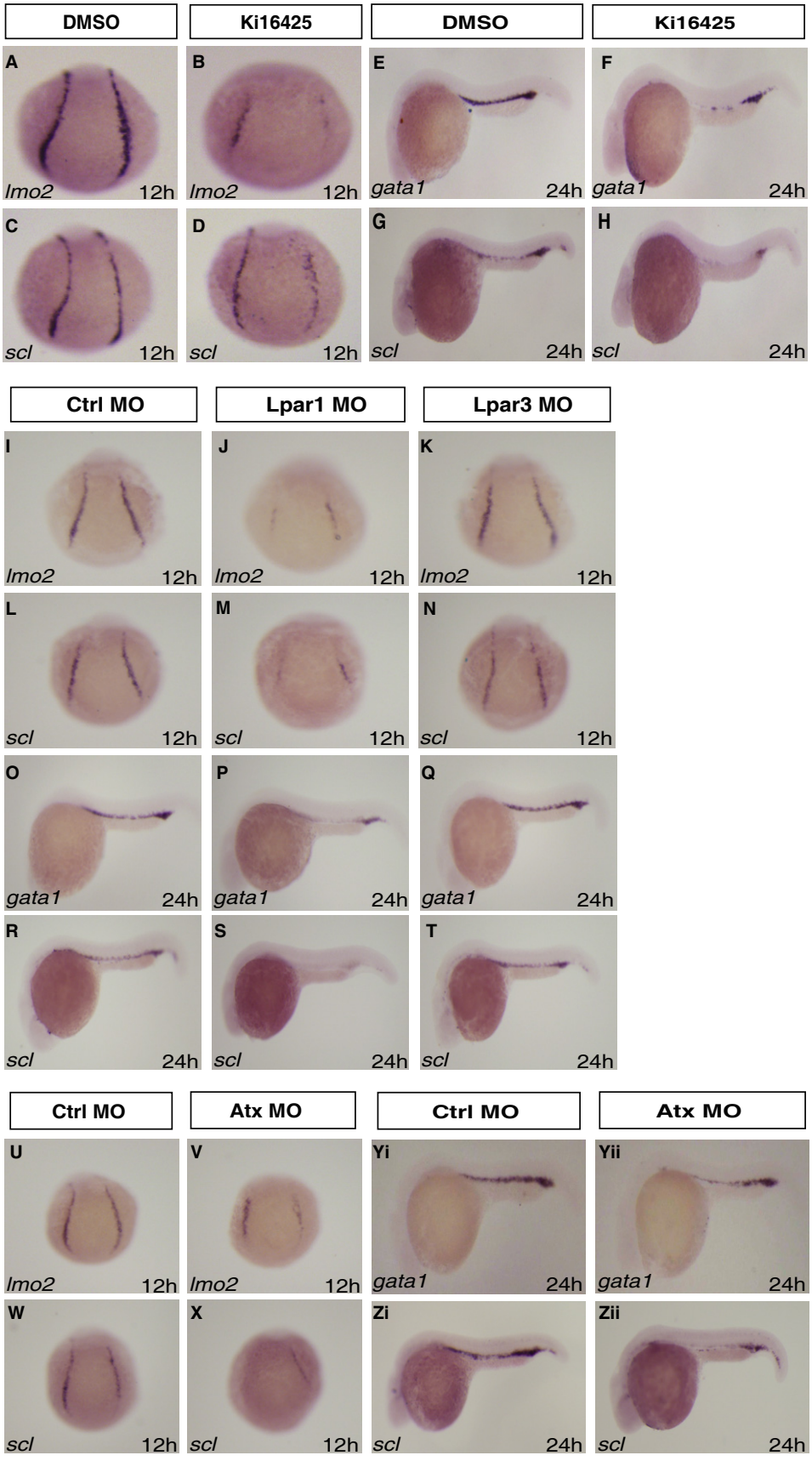

medium was also used for LPA- and ATX-related experiments [0.5 × N2/B27 supplements (Invitrogen), 0.05% BSA, 2 mM glutamine, 0.5 mM ascorbic acid, 4.5 mM monothioglycerol, 10 ng/ml BMP4 (R&D Systems), 20 ng/ml Activin A (PeproTech) with 100 U/ml penicillin and 100 μg/ml streptomycin in IMDM/Ham's F12].

Colony assays

For the hematopoietic progenitor assay, EBs were dissociated by trypsin to single cell suspension and plated in methylcellulose-based medium containing hematopoietic growth factors according to the manufacturer's instructions (M3434; STEMCELL Technologies). Blast cell colonies (BL-CFC) were assayed as previously described (Kennedy *et al*, 1997). Colonies were counted under Olympus CK30-F200 microscope (Olympus, Japan) at 10X objective lense.

Real-time quantitative PCR

Total RNAs were extracted from the whole EBs using TRIzol reagent (Sigma). RNA was reverse transcribed using random hexamers and M-MLV Reverse Transcriptase (Promega). 2 × JumpStart Taq ReadyMix (Sigma) and EvaGreen Dye (Biotium) were used for the PCR reactions, with a Stratagene MX3000P (Agilent Technologies) PCR machine. The relative expression values were normalized against the internal control *gapdh*. Primer sequences are provided in Supplementary Table S1.

Flow cytometry

EB cells were resuspended in PBS containing 1% (wt/vol) BSA. Cells were stained with PE-conjugated anti-FLK1 (555308, BD Biosciences) or APC-conjugated anti-CD41 (17-0411-82, eBioscience) antibody at 1:50 dilution ratio. Propidium iodide (PI; BD Biosciences) was included to exclude the dead cells. Stable mESC lines were constructed by lentivirus transfection and sorted by GFP expression on FACSAria (BD Biosciences). Results were processed using FlowJo software (Tree Star).

Western blotting

The whole EB cell lysates were prepared using 1X Loading Buffer in combination with PhosSTOP (Roche). Samples were then denatured on a heat block at 100°C for 5 minutes. Proteins were resolved by electrophoresis on 8% SDS-PAGE and transferred to nitrocellulose membranes. Membranes were blocked in 5% BSA (1X TBS-Tween20) and probed with the following antibodies: phosphorylated Smad1/5/8 (1:1,000; Cell Signaling), Smad1 (1:1,000; Cell Signaling), Phospho-Akt (Thr308) (1:1,000; Cell Signaling), Phospho-Akt (Ser473) (1:1,000; Cell Signaling), Akt (1:1,000; Cell Signaling), pERK1/2 (1:1,000; Cell Signaling), ERK1/2 (1:1,000; Santa Cruz), and beta-actin (1:1,000; Sigma). The membrane was detected by secondary fluorescent rabbit antibody CW800. The Western blots were quantified using ImageJ (http://imagej.nih.gov/ij/index.html).

Zebrafish maintenance and embryo production

Zebrafish maintenance, breeding, and staging were performed as described previously (Kimmel *et al*, 1995).

Morpholinos, siRNAs, and mRNA synthesis

Morpholino antisense oligonucleotides (MOs) were obtained from Gene Tools. siRNAs were designed and synthesized by GenePharma. The sequence of MO and siRNA is provided in Supplementary Table S2. For generating mRNA, full-length *lpar1* coding sequence was cloned into pCDNA3 vector. To construct EGFP reporters, -213 to +24 bp of *lpar1* gene, which contains the recognition site of *Lpar1* MO, or -61 to +12 bp of *atx* gene, which contains the recognition site of *Atx* MO, was cloned upstream of *EGFP* gene in pcDNA3 vector, respectively. *Lpar1*, *lpar1-EGFP*, and *atx-EGFP* mRNA were synthesized using the mMessage mMachine kit (Ambion).

In vitro RNA synthesis and whole mount *in situ* hybridization

Antisense riboprobes were synthesized using the DIG RNA Labeling kit (Roche) according to the manufacturer's instructions. WISH was performed as previously described (Kissa *et al*, 2008), and staining was performed with an alkaline phosphatase substrate kit (SK-5400, Vector Laboratories, Inc.). Images were captured with Olympus SZX16 microscope fitted with DP71 digital camera, 1X objective lense, and the DP controller acquisition software (Olympus, Japan).

Fluorescence microscopy

Tg*(flk1:EGFP)* transgenic embryos were embedded in 1.0% low melting point agarose for imaging. Images were obtained using Olympus SZX16 system.

Statistical analysis

Quantitative data were expressed as mean ± s.e.m. The statistical significance was analyzed by one-way ANOVA followed by LSD post hoc test for multiple comparisons, or by Student's *t*-test for two comparisons. *P*-value of less than 0.05 was considered statistically significant.

Supplementary information for this article is available online: http://emboj.embopress.org

Acknowledgements

We thank Professor Mien-Chie Hung at the University of Texas MD Anderson Cancer Center for the constitutively active Akt mutant plasmid and Professor Xin Xie for providing small molecule chemicals. We are also grateful to Shunmei Xin, Shiyan Zhou, and Yi Jin for technical assistance. All experiments performed have been authorized by the institutional review board. This work was supported by Chinese Academy of Sciences (XDA01010302), the MOST (2014CB964802), Ministry of Health (2012BAI10B03), Shanghai Municipal Commission for Science and Technology (12ZR1452300), and the National Natural Science Foundation of China (31371419, 31301129).

Author contributions

HL and RY designed and performed the experiments, analyzed the data, and wrote the manuscript; BW analyzed data; GG and JD provided analytical tools; and GP supervised experimental design, data analysis, and manuscript preparation.

Conflict of interest

The authors declare that they have no conflict of interest.

References

Allende ML, Yamashita T, Proia RL (2003) G-protein-coupled receptor S1P1 acts within endothelial cells to regulate vascular maturation. *Blood* 102: 3665 – 3667

Anliker B, Chun J (2004) Lysophospholipid G protein-coupled receptors. *J Biol Chem* 279: 20555 – 20558

Birgbauer E, Chun J (2006) New developments in the biological functions of lysophospholipids. *Cell Mol Life Sci* 63: 2695 – 2701

Chaurio RA, Janko C, Munoz LE, Frey B, Herrmann M, Gaipl US (2009) Phospholipids: key players in apoptosis and immune regulation. *Molecules* 14: 4892 – 4914

Chiang CL, Chen SS, Lee SJ, Tsao KC, Chu PL, Wen CH, Hwang SM, Yao CL, Lee H (2011) Lysophosphatidic acid induces erythropoiesis through activating lysophosphatidic acid receptor 3. *Stem Cells* 29: 1763 – 1773

Choi K, Kennedy M, Kazarov A, Papadimitriou JC, Keller G (1998) A common precursor for hematopoietic and endothelial cells. *Development* 125: 725 – 732

Contos JJ, Fukushima N, Weiner JA, Kaushal D, Chun J (2000) Requirement for the lpA1 lysophosphatidic acid receptor gene in normal suckling behavior. *Proc Natl Acad Sci USA* 97: 13384 – 13389

Cook BD, Liu S, Evans T (2011) Smad1 signaling restricts hematopoietic potential after promoting hemangioblast commitment. *Blood* 117: 6489 – 6497

Damert A, Miquerol L, Gertsenstein M, Risau W, Nagy A (2002) Insufficient VEGFA activity in yolk sac endoderm compromises haematopoietic and endothelial differentiation. *Development* 129: 1881 – 1892

Eilken HM, Nishikawa S, Schroeder T (2009) Continuous single-cell imaging of blood generation from haemogenic endothelium. *Nature* 457: 896 – 900

Ema M, Faloon P, Zhang WJ, Hirashima M, Reid T, Stanford WL, Orkin S, Choi K, Rossant J (2003) Combinatorial effects of Flk1 and Tal1 on vascular and hematopoietic development in the mouse. *Genes Dev* 17: 380 – 393

Estivill-Torrus G, Llebrez-Zayas P, Matas-Rico E, Santin L, Pedraza C, De Diego I, Del Arco I, Fernandez-Llebrez P, Chun J, De Fonseca FR (2008) Absence of LPA1 signaling results in defective cortical development. *Cereb Cortex* 18: 938 – 950

Fehling HJ, Lacaud G, Kubo A, Kennedy M, Robertson S, Keller G, Kouskoff V (2003) Tracking mesoderm induction and its specification to the hemangioblast during embryonic stem cell differentiation. *Development* 130: 4217 – 4227

Feng XH, Derynck R (2005) Specificity and versatility in TGF-beta signaling through Smads. *Annu Rev Cell Dev Biol* 21: 659 – 693

Ferry G, Giganti A, Cogé F, Bertaux F, Thiam K, Boutin JA (2007) Functional invalidation of the autotaxin gene by a single amino acid mutation in mouse is lethal. *FEBS Lett* 581: 3572 – 3578

Fisher MC, Zeisel SH, Mar MH, Sadler TW (2002) Perturbations in choline metabolism cause neural tube defects in mouse embryos *in vitro*. *Faseb J* 16: 619 – 621

Freyer C, Renfree MB (2009) The mammalian yolk sac placenta. *J Exp Zool B Mol Dev Evol* 312: 545 – 554

Fukushima N, Kimura Y, Chun J (1998) A single receptor encoded by vzg-1/lpA1/edg-2 couples to G proteins and mediates multiple cellular responses to lysophosphatidic acid. *Proc Natl Acad Sci USA* 95: 6151 – 6156

Fukushima N, Ishii I, Contos JJ, Weiner JA, Chun J (2001) Lysophospholipid receptors. *Annu Rev Pharmacol Toxicol* 41: 507 – 534

Gadue P, Huber TL, Paddison PJ, Keller GM (2006) Wnt and TGF-beta signaling are required for the induction of an *in vitro* model of primitive streak formation using embryonic stem cells. *Proc Natl Acad Sci USA* 103: 16806 – 16811

Gaengel K, Niaudet C, Hagikura K, Laviña B, Muhl L, Hofmann JJ, Ebarasi L, Nyström S, Rymo S, Chen LL, Pang MF, Jin Y, Raschperger E, Roswall P, Schulte D, Benedito R, Larsson J, Hellström M, Fuxe J, Uhlén P *et al* (2012) The Sphingosine-1-Phosphate Receptor S1PR1 Restricts Sprouting Angiogenesis by Regulating the Interplay between VE-Cadherin and VEGFR2. *Dev Cell* 23: 587 – 599

Gering M, Yamada Y, Rabbitts TH, Patient RK (2003) Lmo2 and SCL/Tal1 convert non-axial mesoderm into haemangioblasts which differentiate into endothelial cells in the absence of Gata1. *Development* 130: 6187 – 6199

Guo F, Jen KL (1995) High-fat feeding during pregnancy and lactation affects offspring metabolism in rats. *Physiol Behav* 57: 681 – 686

Hailesellasse Sene K, Porter CJ, Palidwor G, Perez-Iratxeta C, Muro EM, Campbell PA, Rudnicki MA, Andrade-Navarro MA (2007) Gene function in early mouse embryonic stem cell differentiation. *BMC Genomics* 8: 85

Hales CN, Barker DJ (2001) The thrifty phenotype hypothesis. *Br Med Bull* 60: 5 – 20

Hao J, Ho JN, Lewis JA, Karim KA, Daniels RN, Gentry PR, Hopkins CR, Lindsley CW, Hong CC (2010) *In vivo* structure-activity relationship study of dorsomorphin analogues identifies selective VEGF and BMP inhibitors. *ACS Chem Biol* 5: 245 – 253

Hochman E, Kinston S, Harmelin A, Gottgens B, Izraeli S (2006) The SCL 3′ enhancer responds to Hedgehog signaling during hemangioblast specification. *Exp Hematol* 34: 1643 – 1650

Huber TL, Kouskoff V, Fehling HJ, Palis J, Keller G (2004) Haemangioblast commitment is initiated in the primitive streak of the mouse embryo. *Nature* 432: 625 – 630

Jin X, Yin J, Kim SH, Sohn YW, Beck S, Lim YC, Nam DH, Choi YJ, Kim H (2011) EGFR-AKT-Smad signaling promotes formation of glioma stem-like cells and tumor angiogenesis by ID3-driven cytokine induction. *Cancer Res* 71: 7125 – 7134

Johansson BM, Wiles MV (1995) Evidence for involvement of activin A and bone morphogenetic protein 4 in mammalian mesoderm and hematopoietic development. *Mol Cell Biol* 15: 141 – 151

Kennedy M, Firpo M, Choi K, Wall C, Robertson S, Kabrun N, Keller G (1997) A common precursor for primitive erythropoiesis and definitive haematopoiesis. *Nature* 386: 488 – 493

Khan IY, Dekou V, Douglas G, Jensen R, Hanson MA, Poston L, Taylor PD (2005) A high-fat diet during rat pregnancy or suckling induces cardiovascular dysfunction in adult offspring. *Am J Physiol Regul Integr Comp Physiol* 288: R127 – R133

Kimmel CB, Ballard WW, Kimmel SR, Ullmann B, Schilling TF (1995) Stages of embryonic development of the zebrafish. *Dev Dyn* 203: 253 – 310

Kissa K, Murayama E, Zapata A, Cortes A, Perret E, Machu C, Herbomel P (2008) Live imaging of emerging hematopoietic stem cells and early thymus colonization. *Blood* 111: 1147 – 1156

Koike S, Keino-Masu K, Ohto T, Sugiyama F, Takahashi S, Masu M (2009) Autotaxin/Lysophospholipase D-mediated Lysophosphatidic Acid Signaling Is Required to Form Distinctive Large Lysosomes in the Visceral Endoderm Cells of the Mouse Yolk Sac. *J Biol Chem* 284: 33561 – 33570

Lai SL, Yao WL, Tsao KC, Houben AJ, Albers HM, Ovaa H, Moolenaar WH, Lee SJ (2012) Autotaxin/Lpar3 signaling regulates Kupffer's vesicle formation and left-right asymmetry in zebrafish. *Development* 139: 4439 – 4448

Lancrin C, Sroczynska P, Stephenson C, Allen T, Kouskoff V, Lacaud G (2009) The haemangioblast generates haematopoietic cells through a haemogenic endothelium stage. *Nature* 457: 892 – 895

Lee Z, Cheng CT, Zhang H, Subler MA, Wu J, Mukherjee A, Windle JJ, Chen CK, Fang X (2008) Role of LPA4/p2y9/GPR23 in negative regulation of cell motility. *Mol Biol Cell* 19: 5435 – 5445

Liu Y, Wada R, Yamashita T, Mi Y, Deng CX, Hobson JP, Rosenfeldt HM, Nava VE, Chae SS, Lee MJ, Liu CH, Hla T, Spiegel S, Proia RL (2000) Edg-1, the G protein-coupled receptor for sphingosine-1-phosphate, is essential for vascular maturation. *J Clin Invest* 106: 951 – 961

Liu F, Walmsley M, Rodaway A, Patient R (2008) Fli1 acts at the top of the transcriptional network driving blood and endothelial development. *Curr Biol* 18: 1234 – 1240

Lugus JJ, Chung YS, Mills JC, Kim SI, Grass J, Kyba M, Doherty JM, Bresnick EH, Choi K (2007) Gata2 functions at multiple steps in hemangioblast development and differentiation. *Development* 134: 393 – 405

McKinney-Freeman SL, Naveiras O, Daley GQ (2008) Isolation of hematopoietic stem cells from mouse embryonic stem cells. *Curr Protoc Stem Cell Biol* 4: 1F.3.1 – 1F.3.10

van Meeteren LA, Ruurs P, Stortelers C, Bouwman P, van Rooijen MA, Pradère JP, Pettit TR, Wakelam MJ, Saulnier-Blache JS, Mummery CL, Moolenaar WH, Jonkers J (2006) Autotaxin, a secreted lysophospholipase D, is essential for blood vessel formation during development. *Mol Cell Biol* 26: 5015 – 5022

Mills GB, Moolenaar WH (2003) The emerging role of lysophosphatidic acid in cancer. *Nat Rev Cancer* 3: 582 – 591

Noble RC, Moore JH (1967) The transport of phospholipids from the yolk to the yolk-sac membrane during the development of the chick embryo. *Can J Biochem* 45: 1125 – 1133

Nostro MC, Cheng X, Keller GM, Gadue P (2008) Wnt, activin, and BMP signaling regulate distinct stages in the developmental pathway from embryonic stem cells to blood. *Cell Stem Cell* 2: 60 – 71

Orkin SH, Zon LI (2008) Hematopoiesis: an evolving paradigm for stem cell biology. *Cell* 132: 631 – 644

Park C, Afrikanova I, Chung YS, Zhang WJ, Arentson E, Fong G, Rosendahl A, Choi K (2004) A hierarchical order of factors in the generation of FLK1- and SCL-expressing hematopoietic and endothelial progenitors from embryonic stem cells. *Development* 131: 2749 – 2762

Park C, Lugus JJ, Choi K (2005) Stepwise commitment from embryonic stem to hematopoietic and endothelial cells. *Curr Top Dev Biol* 66: 1 – 36

Qian F, Zhen F, Xu J, Huang M, Li W, Wen Z (2007) Distinct functions for different scl isoforms in zebrafish primitive and definitive hematopoiesis. *PLoS Biol* 5: e132

Rai V, Toure F, Chitayat S, Pei R, Song F, Li Q, Zhang J, Rosario R, Ramasamy R, Chazin WJ, Schmidt AM (2012) Lysophosphatidic acid targets vascular and oncogenic pathways via RAGE signaling. *J Exp Med* 209: 2339 – 2350

Sachinidis A, Gissel C, Nierhoff D, Hippler-Altenburg R, Sauer H, Wartenberg M, Hescheler J (2003) Identification of plateled-derived growth factor-BB as cardiogenesis- inducing factor in mouse embryonic stem cells under serum-free conditions. *Cell Physiol Biochem* 13: 423 – 429

Schmitz G, Ruebsaamen K (2009) Metabolism and atherogenic disease association of lysophosphatidylcholine. *Atherosclerosis* 208: 10 – 18

Soderberg SS, Karlsson G, Karlsson S (2009) Complex and context dependent regulation of hematopoiesis by TGF-beta superfamily signaling. *Ann N Y Acad Sci* 1176: 55 – 69

Tokumura A, Majima E, Kariya Y, Tominaga K, Kogure K, Yasuda K, Fukuzawa K (2002) Identification of human plasma lysophospholipase D, a lysophosphatidic acid-producing enzyme, as autotaxin, a multifunctional phosphodiesterase. *J Biol Chem* 277: 39436 – 39442

Umezu-Goto M, Kishi Y, Taira A, Hama K, Dohmae N, Takio K, Yamori T, Mills GB, Inoue K, Aoki J, Arai H (2002) Autotaxin has lysophospholipase D activity leading to tumor cell growth and motility by lysophosphatidic acid production. *J Cell Biol* 158: 227 – 233

Walmsley M, Cleaver D, Patient R (2008) Fibroblast growth factor controls the timing of Scl, Lmo2, and Runx1 expression during embryonic blood development. *Blood* 111: 1157 – 1166

Warren AJ, Colledge WH, Carlton MB, Evans MJ, Smith AJ, Rabbitts TH (1994) The oncogenic cysteine-rich LIM domain protein rbtn2 is essential for erythroid development. *Cell* 78: 45 – 57

Winnier G, Blessing M, Labosky PA, Hogan BL (1995) Bone morphogenetic protein-4 is required for mesoderm formation and patterning in the mouse. *Genes Dev* 9: 2105 – 2116

Yue R, Li H, Liu H, Li Y, Wei B, Gao G, Jin Y, Liu T, Wei L, Du J, Pei G (2012) Thrombin receptor regulates hematopoiesis and endothelial-to-hematopoietic transition. *Dev Cell* 22: 1092 – 1100

Yukiura H, Hama K, Nakanaga K, Tanaka M, Asaoka Y, Okudaira S, Arima N, Inoue A, Hashimoto T, Arai H, Kawahara A, Nishina H, Aoki J (2011) Autotaxin regulates vascular development via multiple lysophosphatidic acid (LPA) receptors in zebrafish. *J Biol Chem* 286: 43972 – 43983

Zafonte BT, Liu S, Lynch-Kattman M, Torregroza I, Benvenuto L, Kennedy M, Keller G, Evans T (2007) Smad1 expands the hemangioblast population within a limited developmental window. *Blood* 109: 516 – 523

Zhang L, Magli A, Catanese J, Xu Z, Kyba M, Perlingeiro RC (2011) Modulation of TGF-beta signaling by endoglin in murine hemangioblast development and primitive hematopoiesis. *Blood* 118: 88 – 97

